Crystal-Field Effects in $CoCl_2 \cdot 6H_2O$†

NORIKIYO URYÛ,* J. SKALYO, JR.,‡ AND S. A. FRIEDBERG
Carnegie Institute of Technology, Pittsburgh, Pennsylvania
(Received 11 October 1965)

The heat capacities of $CoCl_2 \cdot 6H_2O$ and $NiCl_2 \cdot 6H_2O$ have been measured between 13 and 200°K. The heat capacity of the $CoCl_2 \cdot 6H_2O$ lattice has been estimated from the data on the Ni^{++} salt using a corresponding-states argument and subtracted from the measured total. The remainder is a Schottky anomaly due to the presence of excited Kramers doublets within several hundred cm^{-1} of the lowest one. The doublet separations and g factors of the Co^{++} ion in a crystalline field containing cubic, tetragonal, and rhombic components have been computed as functions of the field parameters and spin-orbit coupling constant. A consistent interpretation of the thermal data and the principal values of the g tensor ($g_1=2.23$, $g_2=5.13$, $g_3=4.90$) deduced from susceptibility measurements is found to require that the crystalline field contain substantial tetragonal and rhombic components. There is an indication that the spin-orbit coupling constant is smaller than the free-ion value.

INTRODUCTION

THE optical absorption spectrum of $CoCl_2 \cdot 6H_2O$ has been investigated above 20°K by Pappalardo.[1] He found that the intensities of certain lines associated with transitions originating in the electronic ground state varied with temperature below 90°K. He suggested as a possible interpretation of this observation, that the ground state might be split by an amount of the order of 100 cm^{-1}. In the absence of information about the structure of this salt, the nature of the electronic ground state was difficult to determine. In his analysis of Pappalardo's data, Koide[2] adopted an ionic model and assumed, on the basis of the known structures of other hexahydrates, that each Co^{2+} ion was probably surrounded by a regular octahedron of six water molecules. Since the ground state of the free Co^{++} ion is ^4F, placing it in the cubic crystalline field produced by these water molecules leaves as the ground state an orbital triplet, Γ_4. The spin degeneracy remains fourfold.

At about this time measurements of the magnetic susceptibility[3–5] of $CoCl_2 \cdot 6H_2O$ revealed it to become antiferromagnetic in the liquid-He region. The Néel point T_N, determined accurately by specific-heat measurements[6,7] to be 2.289°K, was surprisingly high for a salt of this degree of hydration. An explanation of this anomaly was possible after the structure had been determined by Mizuno *et al.*[8] It was found (see Fig. 1) that only four water molecules occupied positions in the octahedral environment of each Co^{++} ion, the two Cl^- ions being located at the two remaining opposite vertices. It was suggested that effective superexchange coupling might occur in this crystal via paths involving these specially situated Cl^- ions. The presence of the Cl^- ions also insures that the crystalline electric field at each Co^{++} ion will contain components other than cubic. It is thus quite likely that the orbital angular momentum of the ground state of the Co^{++} ion in $CoCl_2 \cdot 6H_2O$ is actually quenched. Since the heat capacity data show that the ground state is doubly degenerate, we infer that it is a Kramers spin doublet. The first excited levels, suggested by Pappalardo to lie ~ 100 cm^{-1} above the lowest ones, are then expected to be a second Kramers doublet, i.e., the remaining spin components of the lowest orbital state.

The energy separation of the first excited Kramers doublet from the lowest one depends, of course, on the symmetry and strength of the crystalline field as well as on the magnitude of the spin-orbit coupling constant. The existing optical data do not provide quantitative

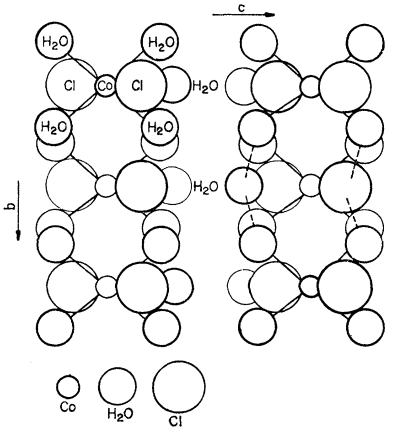

FIG. 1. Structure of $CoCl_2 \cdot 6H_2O$ projected on (100) according to Mizuno *et al.* (Ref. 8). The crystal is monoclinic with $\beta=122°\ 19'$ and belongs to the space group C_{2h}^3-C2/m. There are two formula units per unit cell.

† Work supported by the National Science Foundation and the U. S. Office of Naval Research.

* Present address: Department of Applied Science, Faculty of Engineering, Kyushu University, Fukuoka, Japan.

‡ Present address: Los Alamos Scientific Laboratory, Los Alamos, New Mexico.

[1] R. Pappalardo, Phil. Mag. **4**, 219 (1959).

[2] S. Koide, Phil. Mag. **4**, 243 (1959).

[3] T. Haseda and E. Kanda, J. Phys. Soc. Japan **12**, 1051 (1959).

[4] R. B. Flippen and S. A. Friedberg, J. Appl. Phys. **31**, 338S (1960).

[5] T. Haseda, J. Phys. Soc. Japan **15**, 483 (1960).

[6] W. K. Robinson and S. A. Friedberg, Phys. Rev. **117**, 402 (1960).

[7] J. Skalyo, Jr., and S. A. Friedberg, Phys. Rev. Letters **13**, 133 (1964).

[8] J. Mizuno, K. Ukei, and T. Sugawara, J. Phys. Soc. Japan **14**, 383 (1959); J. Mizuno, *ibid.* **16**, 1574 (1961).

TABLE I. Heat capacity of $CoCl_2 \cdot 6H_2O$. Temperature is in °K and C_p is in cal/°K mole.

T	C_p	T	C_p	T	C_p	T	C_p
13.21	0.97	54.58	16.96	111.77	36.11	160.43	48.35
14.09	1.13	55.09	17.03	113.18	36.35	162.33	48.74
15.31	1.41	56.65	17.50	114.55	36.94	164.09	49.26
16.47	1.65	58.11	18.22	115.88	37.18	165.78	49.67
17.86	2.01	59.52	18.77	117.18	37.39	167.37	49.91
19.15	2.40	63.75	20.64	118.43	37.88	168.92	50.34
20.03	2.64	65.08	21.21	119.65	37.97	170.39	51.22
20.94	2.88	66.36	21.51	120.85	38.54	171.76	52.50
21.92	3.33	67.59	22.17	122.20	38.71	173.11	52.06
22.74	3.73	68.88	22.32	123.63	39.55	174.41	52.91
23.46	3.82	70.18	23.02	124.96	39.46	175.58	52.96
24.12	3.93	71.45	23.54	126.23	40.15	176.70	52.58
24.80	4.24	76.20	25.10	127.48	40.28	178.25	52.59
25.58	4.46	77.88	25.65	127.25	40.42	180.03	53.53
26.38	4.74	79.41	25.95	128.73	40.45	181.39	53.48
27.38	5.19	80.45	26.47	129.59	40.83	183.27	52.75
28.57	5.69	81.51	26.97	131.07	41.17	185.03	54.20
29.59	6.07	85.82	28.38	132.50	41.19	187.01	54.82
31.13	6.76	86.94	28.82	133.96	41.29	188.76	54.68
33.18	7.68	88.04	29.29	135.42	41.86	190.03	52.82
36.03	8.82	89.47	29.65	136.90	42.20	191.95	54.24
40.48	10.72	91.18	30.01	138.33	42.89	192.32	56.04
42.16	11.37	92.84	30.26	139.72	43.19	193.48	54.14
43.71	11.95	94.38	31.04	141.10	43.17	194.36	56.81
45.11	12.80	95.95	31.52	144.24	44.36	194.85	55.18
46.38	13.48	97.15	31.87	145.89	44.85	196.11	58.39
47.57	13.93	97.43	31.77	147.50	45.00	196.14	57.36
48.94	14.36	98.65	32.17	149.05	45.84	197.26	55.65
49.39	14.88	100.10	32.74	150.59	46.63	198.01	58.89
50.34	15.52	101.72	33.16	153.05	46.58	198.30	56.75
50.49	15.12	103.47	33.92	154.29	46.91	199.09	59.41
51.61	15.85	105.20	34.32	155.65	47.04	199.59	56.83
51.92	15.78	106.87	34.70	156.59	48.07	199.99	59.34
53.13	16.70	108.42	35.21	158.46	48.28	200.80	60.21
53.48	16.51	109.98	35.88				

information about this separation. Even were the separation accurately known, it would not be sufficient alone to determine all of the parameters required to specify the crystalline field and spin-orbit coupling constants.

Other properties of the solid depending upon these parameters include the spectroscopic splitting or g factors. Knowing the g factors from paramagnetic resonance or susceptibility measurements, as well as the doublet separations, it should be possible to determine all of the constants of interest. In principle, g factors are best determined by resonance methods. This is usually done with specimens diluted with a diamagnetic isomorph of the salt. Unfortunately, the only known isomorph of $CoCl_2 \cdot 6H_2O$ is $NiCl_2 \cdot 6H_2O$, so that the only paramagnetic resonance data available have had to be obtained with the concentrated material. Date[9] has measured the g factors at temperatures slightly above T_N and has noted the possible effect on their magnitudes of short-range magnetic ordering in this region. The least ambiguous values thus appear to be those calculated from the Curie constants determined by susceptibility measurements in the liquid-hydrogen range. The results of Flippen and Friedberg[4] and of Haseda[5] are in reasonable agreement and yield $g_b = 5.0(4.9)$, $g_c = 4.9(4.9)$, $g_{a'} = 2.7(2.9)$. The directions b and c are axes in the monoclinic system according to Groth's[10] designation. The direction a' is in the a-c plane and is orthogonal to both b and c. It is inclined about 32° from the a direction since $\beta = 122° 19'$. As we shall see later, supplementary data in the a-c plane are required to determine the principal values of the g tensor.

The accurate determination of the separation of the lowest and first excited Kramers doublets could presumably be accomplished by optical absorption measurements in the extreme infrared. To our knowledge such measurements have not been performed on this or other hydrated crystals. We have considered other possible methods. The fact[8] that $CoCl_2 \cdot 6H_2O$ is isostructural with $NiCl_2 \cdot 6H_2O$ suggests that thermal measurements may be capable of giving the desired information. The lattice heat capacities of these two substances, whose ionic masses are practically identical, are nearly the same.[6] Since the Ni^{++} ion in $NiCl_2 \cdot 6H_2O$ has no low-lying excited electronic states near the ${}^3A(\Gamma_2)$ ground state, we can use the heat capacity of this salt above ~ 20°K as a measure of the lattice heat capacity of $CoCl_2 \cdot 6H_2O$ in the same region. Subtracting this correction from the measured total heat capacity of $CoCl_2 \cdot 6H_2O$, we should expect the remainder to be a Schottky "bump" whose details depend on the separa-

[9] M. Date, J. Phys. Soc. Japan **16**, 1337 (1961).

[10] P. Groth, *Chemische Krystallographie*, (Engelmann, Leipzig 1906), Teil I, p. 248.

TABLE II. Heat capacity of $NiCl_2 \cdot 6H_2O$. Temperature is in °K and C_p is in cal/°K mole.

T	C_p	T	C_p	T	C_p	T	C_p
13.52	1.10	62.10	18.54	95.76	30.35	129.37	39.83
14.67	1.29	63.38	19.00	97.00	31.00	131.40	39.81
15.57	1.48	64.70	19.43	90.23	28.16	133.29	40.19
16.68	1.72	64.79	19.23	91.54	28.81	135.10	40.09
17.94	2.00	65.92	20.02	92.80	29.13	136.78	41.61
19.08	2.25	66.14	20.16	94.01	29.99	138.53	41.27
20.14	2.51	67.12	20.37	95.19	30.03	140.47	41.92
20.90	2.72	67.43	20.45	96.31	30.22	142.29	42.63
22.01	3.02	68.28	20.77	97.40	30.61	144.00	42.26
22.99	3.23	69.40	21.17	98.46	31.13	145.54	43.26
23.91	3.89	70.50	21.63	99.50	31.81	147.08	43.76
24.89	3.99	71.84	22.09	101.10	31.40	148.85	44.14
25.69	4.60	73.16	22.67	102.95	32.21	150.52	44.28
27.01	4.72	74.43	23.33	104.72	32.47	152.01	45.08
28.44	5.15	75.66	23.70	106.40	33.49	153.06	44.90
29.45	5.56	76.87	23.98	107.70	33.48	154.88	45.37
30.43	6.10	78.00	24.45	108.78	34.07	156.53	46.33
31.28	6.35	78.29	24.27	109.92	34.54	158.07	46.29
32.42	6.86	79.13	24.72	108.03	33.57	159.85	46.31
33.53	7.21	79.56	24.67	110.99	34.50	161.72	47.50
35.01	7.98	80.18	24.89	112.02	34.56	163.49	48.24
37.10	8.90	80.79	25.01	113.00	35.19	165.09	49.29
38.93	9.69	81.42	25.51	113.94	35.15	166.54	50.40
40.57	10.19	82.86	25.92	119.08	35.98	168.12	50.10
42.49	10.94	82.93	25.94	110.12	33.97	169.93	50.50
44.02	11.48	84.04	26.13	112.02	34.83	171.56	50.75
46.62	12.49	84.19	26.58	112.39	34.82	173.05	51.49
49.85	13.53	85.07	2o.48	114.65	35.31	186.22	51.26
51.27	14.14	86.10	27.13	116.81	36.14	187.66	52.70
53.55	15.03	87.10	27.25	118.88	36.37	188.92	52.41
54.74	15.88	88.05	27.37	120.82	37.13	190.94	52.48
55.85	16.16	90.70	28.92	121.29	36.24	192.74	53.95
56.94	16.47	91.99	29.31	122.69	37.43	194.30	55.82
58.00	16.94	93.26	29.72	123.22	37.84	195.64	56.88
58.96	17.32	93.77	29.10	125.00	37.77	196.86	56.33
59.90	17.22	94.52	30.30	125.09	37.95	197.84	56.01
60.99	17.85	94.86	29.63	127.24	38.45		

tion of the first and second Kramers doublets. Higher excited states might also influence this "bump" if close enough in energy.

As a first step in this program, we have measured the heat capacities of $CoCl_2 \cdot 6H_2O$ and $NiCl_2 \cdot 6H_2O$ between 13 and 200°K, as will be described below. The experimental results have been analyzed as suggested with the added refinement that the $NiCl_2 \cdot 6H_2O$ data have been adjusted by a corresponding states argument to give a closer approximation to the lattice heat capacity of $CoCl_2 \cdot 6H_2O$.

The experimental phase of the present work has included also the performance of additional magnetic susceptibility measurements on single crystal $CoCl_2 \cdot 6H_2O$ in its *a-c* plane. These measurements have been performed as described in Ref. 4 and will be quoted later.

The theoretical study of the Co^{++} ion in $CoCl_2 \cdot 6H_2O$ constitutes the major portion of the present paper. The theory of the level splittings and g factors has been developed in detail from the point of view of an ionic model. While the occurrence of antiferromagnetism below $T_N = 2.289$°K clearly indicates the presence of significant exchange interaction, this interaction is sufficiently small in comparison with the level separations of interest that it may be ignored in these calculations. As will be shown below, a consistent picture of the relevant properties of $CoCl_2 \cdot 6H_2O$ is obtained only when the crystalline field at a Co^{++} ion is assumed to contain significant axial and rhombic components in addition to the cubic part. The origin of these components will be considered briefly.

CALORIMETRIC EXPERIMENTS

The heat capacities of $CoCl_2 \cdot 6H_2O$ have been measured between 13 and 200°K in a simple vacuum calorimeter.[11] The specimens, in the form of small crystals, were contained in a copper capsule to which were attached a calibrated Leeds and Northrup platinum resistance thermometer and a manganin heater winding. Helium gas, sealed under reduced pressure inside the capsule together with the specimen material, insured the rapid attainment of thermal equilibrium. A discontinuous heating procedure was employed. The heat capacity of the empty capsule was determined in a separate series of experiments.

The specimens of both materials were prepared from analytical quality "Certified Reagents" obtained from

[11] Similar in most respects to that described by I. Estermann and J. R. Weertman, J. Chem. Phys. **20**, 972 (1952).

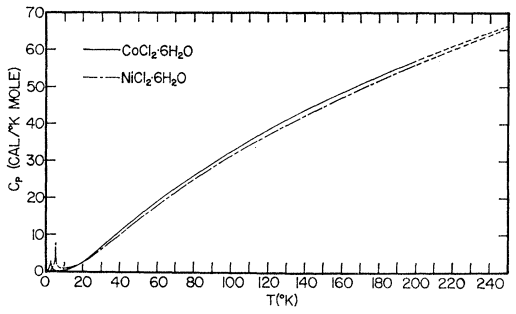

FIG. 2. The heat capacities C_p of $CoCl_2 \cdot 6H_2O$ and $NiCl_2 \cdot 6H_2O$ versus temperature.

the Fisher Scientific Supply Company. The maximum impurity content of these materials is given in Ref. 6, the earlier measurements below 20°K having been performed on similar specimens. The $CoCl_2 \cdot 6H_2O$ sample weighed 7.983 g (0.03355 moles) while the $NiCl_2 \cdot 6H_2O$ sample weighed 7.077 g (0.02977 moles).

The measured heat capacities of $CoCl_2 \cdot 6H_2O$ and $NiCl_2 \cdot 6H_2O$ between 13 and 200°K are summarized in Tables I and II. Over most of this range the spread of the data does not exceed 1 or 2%. Above about 170°K the experimental uncertainty begins to grow significantly larger due to difficulty in achieving thermal isolation in the relatively simple calorimeter employed in this work. Data reliable only to within about 10% have been obtained between 200°K and room temperature. They have been included as dashed portions of the smoothed curves of C_p versus T displayed in Fig. 2 which also includes earlier results obtained between 1.4 and 20°K. In the range 13 to 20°K these two independent sets of experiments on specimens of quite different size are in excellent agreement.

The fact that C_p of $CoCl_2 \cdot 6H_2O$ exceeds that of $NiCl_2 \cdot 6H_2O$ at temperatures not very far above the cooperative anomalies characterizing their Néel points, suggests immediately the presence of low-lying excited states of the Co^{++} ion. The isolation of the contribution of these states to the heat capacity of $CoCl_2 \cdot 6H_2O$ has proceeded in two steps. First, the cooperative anomalies have been subtracted from $C_p - T$ curves for both salts thus removing the contributions arising from the spin components of the Ni^{++} and Co^{++} ground states. This process has been facilitated by the fact that from ~15°K down to a temperature very near T_N, the total heat capacity of each salt could be well represented by a relation[6] $C_p/R = AT^3 + B/T^2$. The first term gives a reasonable approximation to the lattice heat capacity at temperatures up to ~15°K. The term in T^{-2} represents the high-temperature paramagnetic "tail" of the cooperative anomaly and may be reliably extrapolated until it becomes negligibly small.

Finally, an estimate of the lattice heat capacity must be subtracted from the corrected $CoCl_2 \cdot 6H_2O$ data. As a first approximation to the lattice contribution, we have simply used a smooth curve drawn through the corrected $NiCl_2 \cdot 6H_2O$ data. The result is given in Fig. 3 (circles) and clearly exhibits the general form of a Schottky anomaly having its maximum at about 100°K. As will be shown below, there is good reason to believe that the lattice correction is underestimated in this simplified treatment. Seeking an improved lattice correction, we have adopted a procedure similar to that used by Stout and Catalano[12] in an analogous problem. We assume that the lattice contributions to the heat capacities of $CoCl_2 \cdot 6H_2O$ and $NiCl_2 \cdot 6H_2O$ obey a law of corresponding states. Thus $C_p(\text{lat.}) = f(T/\theta)$, where f is the same function for both salts and θ is a constant characteristic of a given salt. At some temperature T', the lattice heat capacity of the Co salt C_p(lat., Co) is the same as that of the Ni salt at another temperature T''. Thus $T''/T' = \theta(\text{Ni})/\theta(\text{Co}) = r$. The lattice heat capacity of the Co salt may thus be written at any temperature T

$$C_p(\text{lat., Co}) = f\{T/\theta(\text{Co})\} = f\{rT/\theta(\text{Ni})\}, \quad (1)$$

i.e., the lattice heat capacity of $CoCl_2 \cdot 6H_2O$ at T should be that of $NiCl_2 \cdot 6H_2O$ at a temperature rT. The factor r may be determined from the T^3 laws obeyed by the lattice heat capacities of both salts below ~15°K, i.e., in a region where the principle of corresponding states is clearly valid. We find $r = 1.018$ and so the lattice correction is larger at a given temperature than it was in the simplified approximation.

The result of making the corresponding states adjustment of the smooth curve drawn through the $NiCl_2 \cdot 6H_2O$ data before subtracting it from the $CoCl_2 \cdot 6H_2O$ is shown in Fig. 3 (crosses). Again the electronic excess heat capacity of the $CoCl_2 \cdot 6H_2O$ exhibits a Schottky curve but the maximum is now lower in both magnitude and temperature (~83°K). Vertical bars have been drawn to indicate the maximum possible errors in these heat capacity values. Because of the fact that we are taking differences of large numbers, these uncertainties quickly become very large as the temperature is raised. It is rather clear, however, that low-lying

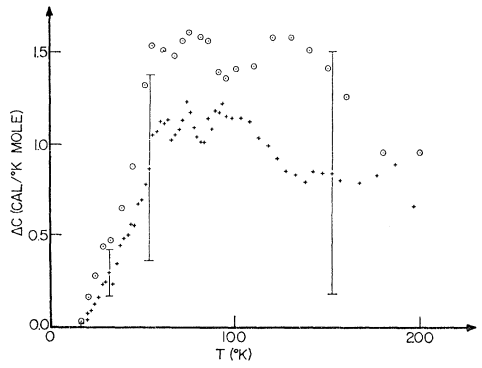

FIG. 3. The electronic excess heat capacity of $CoCl_2 \cdot 6H_2O$, the lattice correction having been made by the subtraction of (1) smoothed $NiCl_2 \cdot 6H_2O$ data (circles) and (2) $NiCl_2 \cdot 6H_2O$ data adjusted by corresponding states argument (crosses).

[12] J. W. Stout and E. Catalano, J. Chem. Phys. 23, 2013 (1955).

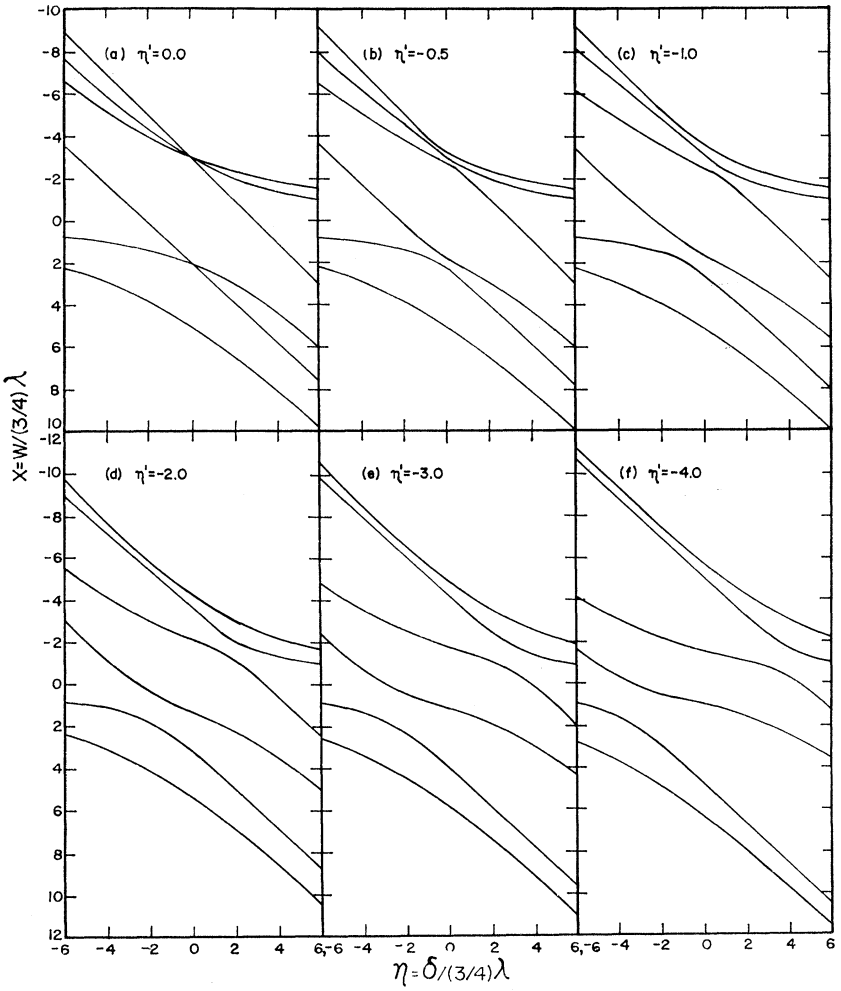

FIG. 4. The variation of the reduced energy, $x=W/(\frac{3}{4})\lambda$, of the six lowest Kramers doublets of Co^{++} with reduced tetragonal crystalline field parameter η for several values of the reduced rhombic crystalline field parameter η'.

excited states of the Co^{++} ion have been detected thermally and that they are located at roughly the energies required to explain the intensity variation observed with temperature in Pappalardo's optical data. Quantitative use will be made of these results in the concluding discussion.

THEORY OF Co^{++} IN A CRYSTALLINE FIELD OF LOW SYMMETRY

Theoretical investigation of the effects of the crystalline field on a Co^{++} ion has been carried out by Abragam and Pryce[13] for two important cases. In treating the Co-Tutton salt, they have considered the field to possess cubic and tetragonal components; for Co-fluosilicate, the field has been assumed to contain cubic and trigonal parts. In both cases they have calculated the splitting of the electronic energy levels arising from the free-ion ^4F state taking into account the effects of the excited ^4P state and have studied the variation of the g factors with crystalline field parameters.

Kambe *et al.*[14] have also discussed the effects of combined cubic and tetragonal crystalline fields on a Co^{++} ion in Co-Tutton salt. The results of their calculations of the energy levels and g factors as functions of a suitable parameter describing the tetragonal crystalline field and defined below are reproduced in Figs. 4(a) and 5(a).

As mentioned in the introduction, the g factors obtained from previous susceptibility measurements on $CoCl_2 \cdot 6H_2O$ are $g_b=5.0(4.9)$, $g_c=4.9(4.9)$, and $g_{a'}=2.7(2.9)$. These values suggest that the macroscopic and microscopic symmetry may be tetragonal. At first sight this seems to be consistent with the structure of the local environment of a Co^{++} ion in Fig. 1. The tetragonal axis would appear to coincide with the line joining two Cl^- ions at opposite vertices of the octahedron of surrounding ligands. Adopting this view and using the results of Fig. 5(a), Haseda[5] has noted that $g_{\parallel}=2.9$ and $g_{\perp}=4.9$ imply an η value of about -4.0.

However, there is no physical reason to consider the

[13] A. Abragam and M. H. L. Pryce, Proc. Roy. Soc. (London) **A206**, 173 (1951).

[14] K. Kambe, S. Koide, and T. Usui, Progr. Theoret. Phys. (Kyoto) **7**, 15 (1952).

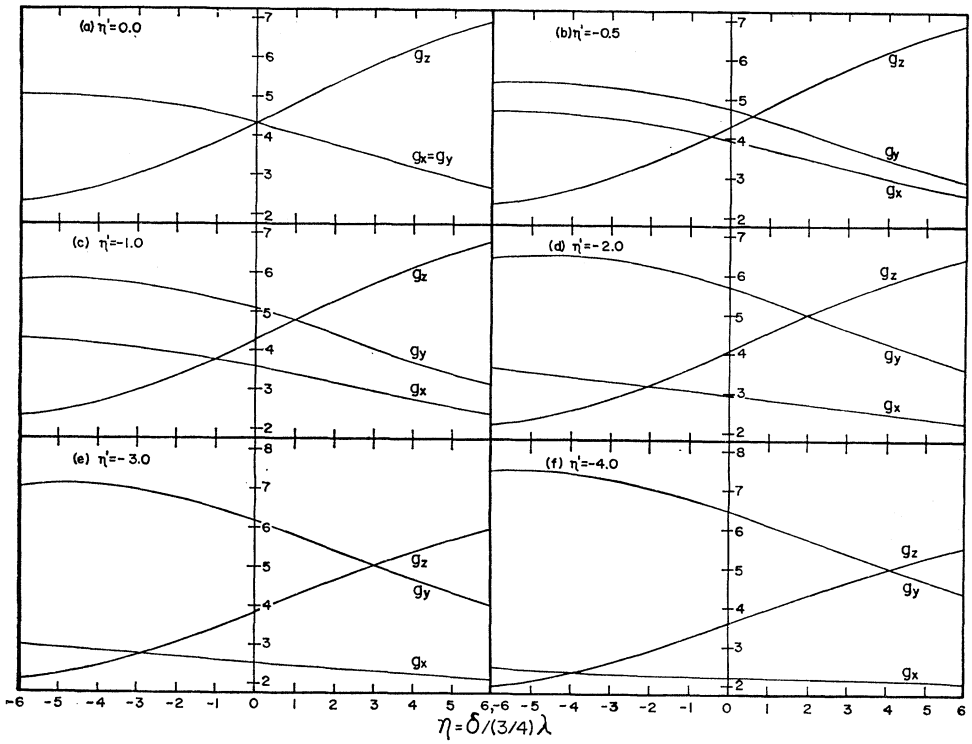

FIG. 5. The variation of the principal values of the g tensor with reduced tetragonal crystalline field parameter η for several values of the reduced rhombic crystalline field parameter η'.

b, c, and a' directions all to coincide with principal axes of the g tensor. The monoclinic symmetry of the crystal requires only that the b or diad axis be a principal axis, the other two being required merely to lie in the a-c plane at right angles to one another and to b. Note in Fig. 1 that the b axis is actually perpendicular to the $Cl^- - Cl^-$ direction. Thus, it is not necessary that the latter direction coincide with a principal axis of the g tensor. The two H_2O molecules not belonging to the immediate environment of the Co^{++} ion are, nevertheless, quite close to it. Together with the other four H_2O molecules, they may be considered to form a second distorted octahedron about the Co^{++} ion and may add a small orthorhombic part to the cubic and tetragonal components of the crystalline field. The inclusion of this component affects only the principal axes in the a-c plane since the b axis retains its privileged character. As will be evident below, $g_{a'}=2.7$ and $g_c=4.9$ can be realized in several ways if the principal axes of the g tensor deviate from c and a' in the presence of a crystalline field of orthorhombic symmetry.

As far as it affects atomic d-electrons, the crystalline field potential can be written in the following form:

$$V=e\sum_i [A(x_i^2+y_i^2-2z_i^2)+B(x_i^2-y_i^2)+D(x_i^4+y_i^4+z_i^4)+Q(z_i^4+6x_i^2y_i^2)+f(r_i)], \quad (2)$$

where A, B, D, Q, and $f(r)$ are functions of r. Here the tetragonal axis has been taken as the z axis. The first and the fourth terms represent the tetragonal field components and the third term, the cubic component. The second term appears as a result of the introduction of an orthorhombic field component. For the sake of simplicity, we have taken here the orthorhombic term of the second degree and omitted the term of the fourth degree. However, this will be enough to enable us to see the effects of the orthorhombic component.

The lowest orbital state ^4F of the free Co^{++} ion splits into two triplets, Γ_4 and Γ_5, and a singlet Γ_2 in a crystalline field of cubic symmetry with Γ_4 lowest. The energy separation between the ground state Γ_4 and the first excited orbital state Γ_5 is given by $(104/21)e\langle Dr^4\rangle_{av}$ and is of the order of 10^4 cm^{-1}. For the present purpose it will be sufficient to consider the lowest orbital state, Γ_4, alone.

The three orbital states included in Γ_4 are given by the following wave functions:

$$\langle 0| = \varphi_0, \quad (3a)$$

$$\langle 1| = \tfrac{1}{4}[(\sqrt{10})\varphi_3+(\sqrt{6})\varphi_{-1}], \quad (3b)$$

$$\langle 2| = \tfrac{1}{4}[(\sqrt{6})\varphi_1+(\sqrt{10})\varphi_{-3}], \quad (3c)$$

where φ_{M_L} ($M_L=\pm3, \pm2, \pm1, 0$) is the orbital wave function with the magnetic quantum number M_L ($L=3$). The lowest orbital state has a fourfold spin degeneracy. Therefore, under the combined action of the tetragonal field, orthorhombic field, and the spin-orbit coupling, the lowest state splits into six doublets.

We can conveniently use the method of operator equivalents[15] for the calculation of the matrix elements

[15] K. W. H. Stevens, Proc. Phys. Soc. (London) **A65**, 209 (1952).

of V. Equivalent operators for each term of Eq. (2) are given as follows:

$$e\sum_i A(x_i^2+y_i^2-2z_i^2)=-\alpha e\langle Ar^2\rangle_{\rm av}\{3L_z^2-L(L+1)\},$$

$$e\sum_i B(x_i^2-y_i^2)=\tfrac{1}{2}\alpha e\langle Br^2\rangle_{\rm av}(L_+^2+L_-^2),$$

$$e\sum_i D(x_i^4+y_i^4+z_i^4-\tfrac{3}{5}r_i^4)$$
$$=e\beta\langle Dr^4\rangle_{\rm av}\{(1/20)[35L_z^4-30L(L+1)L_z^2$$
$$+25L_z^2-6L(L+1)+3L^2(L+1)^2]+\tfrac{1}{8}[L_+^4+L_-^4]\},$$

$$e\sum_i Q(z_i^4+6x_i^2y_i^2)$$
$$=e\beta\langle Qr^4\rangle_{\rm av}\{\tfrac{3}{4}L^2(L+1)^2+(5/4)L_z^2+(7/4)L_z^4$$
$$-\tfrac{1}{2}L(L+1)(3L_z^2+1)-\tfrac{3}{8}(L_+^4+L_-^4)\},$$

where the average $\langle\ \rangle_{\rm av}$ is to be taken over the density of the $3d$-atomic orbital, and the coefficients α and β are given as $\alpha=-2/105$ and $\beta=-2/315$, respectively, for the case of $d^7(^4F)$.

When the spin-orbit interaction $\lambda\mathbf{L}\cdot\mathbf{S}$ and the crystalline field potential V are taken as perturbations on the free Co^{++} ion, the 12×12 secular matrix can be decomposed into two 6×6 matrices as follows:

$$\begin{array}{cccccc}
|1,\tfrac{3}{2}\rangle & |1,-\tfrac{1}{2}\rangle & |2,\tfrac{3}{2}\rangle & |2,-\tfrac{1}{2}\rangle & |0,\tfrac{1}{2}\rangle & |0,-\tfrac{3}{2}\rangle \\
|2,-\tfrac{3}{2}\rangle & |2,\tfrac{1}{2}\rangle & |1,-\tfrac{3}{2}\rangle & |1,\tfrac{1}{2}\rangle & |0,-\tfrac{1}{2}\rangle & |0,\tfrac{3}{2}\rangle \\
\left(\begin{array}{cccccc}
(9/4)\lambda+\delta & 0 & \tfrac{3}{4}\delta' & 0 & (3\times6^{1/2}/4)\lambda & 0 \\
0 & -\tfrac{3}{4}\lambda+\delta & 0 & \tfrac{3}{4}\delta' & 0 & (3\times6^{1/2}/4)\lambda \\
\tfrac{3}{4}\delta' & 0 & -(9/4)\lambda+\delta & 0 & 0 & 0 \\
0 & \tfrac{3}{4}\delta' & 0 & \tfrac{3}{4}\lambda+\delta & \tfrac{3}{2}\sqrt{2}\lambda & 0 \\
(3\times6^{1/2}/4)\lambda & 0 & 0 & \tfrac{3}{2}\sqrt{2}\lambda & 0 & 0 \\
0 & (3\times6^{1/2}/4)\lambda & 0 & 0 & 0 & 0
\end{array}\right)
\end{array}, \qquad (4)$$

In this secular matrix, we have omitted from the diagonal elements the common term $12e\alpha\langle Ar^2\rangle_{\rm av}+102e\beta\langle Qr^4\rangle_{\rm av}+18e\beta\langle Dr^4\rangle_{\rm av}$, and δ and δ' are given by the following expressions:

$$\delta=(10/35)e\langle Qr^4\rangle_{\rm av}+(12/35)e\langle Ar^2\rangle_{\rm av},$$
$$\delta'=-(4/35)e\langle Br^2\rangle_{\rm av}.$$

The unperturbed eigenfunctions $|1,\tfrac{3}{2}\rangle$, $\cdots$, etc., are the products, for example, of the orbital wave function $|1\rangle$ and the spin eigenfunction $u(\tfrac{3}{2})$ with $M_s=+\tfrac{3}{2}$, i.e.,

$$|1,\tfrac{3}{2}\rangle=|1\rangle u(\tfrac{3}{2}),\ \text{etc.}$$

As in the case treated by Kambe *et al.*, if we measure the energy level W in units of $(\tfrac{3}{4})\lambda(=-135\ \text{cm}^{-1})$ and write $\delta/(\tfrac{3}{4})\lambda=\eta$, $\delta'/(\tfrac{3}{4})\lambda=\eta'$, we can obtain the reduced energy eigenvalue $x(=W/(\tfrac{3}{4})\lambda)$ as a function of η and η'. This has been done with the Bendix G20 computer. In Fig. 4, the results obtained are summarized by drawing the variation of x as a function of η for some selected values of η'.

In order to calculate the g factor of the lowest level, the first-order Zeeman splitting ΔW must be obtained. The wave functions of the lowest level are

$$\Psi_1=C_1|1,\tfrac{3}{2}\rangle+C_2|1,-\tfrac{1}{2}\rangle+C_3|2,\tfrac{3}{2}\rangle+C_4|2,-\tfrac{1}{2}\rangle$$
$$+C_5|0,\tfrac{1}{2}\rangle+C_6|0,-\tfrac{3}{2}\rangle, \qquad (5a)$$

$$\Psi_2=C_1|2,-\tfrac{3}{2}\rangle+C_2|2,\tfrac{1}{2}\rangle+C_3|1,-\tfrac{3}{2}\rangle+C_4|1,\tfrac{1}{2}\rangle$$
$$+C_5|0,-\tfrac{1}{2}\rangle+C_6|0,\tfrac{3}{2}\rangle. \qquad (5b)$$

If we denote by H the magnitude of the external magnetic field, $\Delta W=g\mu_B H$. When the external magnetic field is applied in the direction of the z axis, the matrix elements of $H_m=\mu_B H_z(L_z+2S_z)$ are obtained as follows:

$$(\Psi_1|H_m|\Psi_1)=-(\Psi_2|H_m|\Psi_2)$$
$$=\mu_B H_z\{\tfrac{9}{2}C_1^2+\tfrac{1}{2}C_2^2+\tfrac{3}{2}C_3^2$$
$$-\tfrac{5}{2}C_4^2+C_5^2-3C_6^2\},$$
$$(\Psi_1|H_m|\Psi_2)=(\Psi_2|H_m|\Psi_1)=0,$$

whence the g value is

$$g_z=9C_1^2+C_2^2+3C_3^2-5C_4^2+2C_5^2-6C_6^2. \qquad (6a)$$

Similarly, for the field along the x or y axis, the g values are found to be

$$g_x=3\sqrt{2}(C_1C_6+C_2C_5+C_3C_6+C_4C_5)$$
$$+4\sqrt{2}(C_1C_4+C_2C_3+C_5C_6)+8C_2C_4+8C_5^2, \qquad (6b)$$

$$g_y=3\sqrt{2}(-C_1C_6-C_2C_5+C_3C_6+C_4C_5)$$
$$+4\sqrt{3}(C_1C_4+C_2C_3-C_5C_6)-8C_2C_4+4C_5^2. \qquad (6c)$$

The coefficients C_i of the ground-state wave functions (5a), (5b) may be obtained as functions of η and η' using the secular matrix (4) and the lowest energy eigenvalue. For several values of η', g_x, g_y, and g_z have been calculated as functions of η and the results plotted in Fig. 5.

DISCUSSION

As has been mentioned in the previous section, it is quite likely that the crystalline field at the Co^{++} ion in

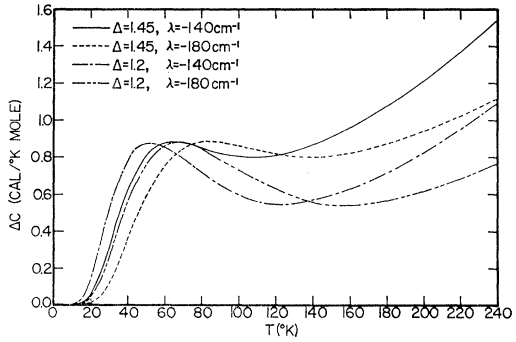

FIG. 6. Computed electronic heat capacity of Co^{++} ions for two values of spin-orbit coupling constant $\lambda=-140$ cm^{-1} and $\lambda=-180$ cm^{-1}. $\Delta=1.45$ corresponds to $\eta=3.25$ and $\eta'=-3$, while $\Delta=1.2$ corresponds to $\eta=3.75$ and $\eta'=-4$.

$CoCl_2\cdot 6H_2O$ contains a rhombic component and that the a' and c axes are not principal axes of the g tensor. This conjecture has been confirmed by measurements of the susceptibility along a direction in the a-c plane (d direction) making an angle of 45° with the a' and c axes. These measurements were kindly carried out for us by Mrs. S. Barros between 14 and 20°K. They yielded a Curie-Weiss law from which one obtains a splitting factor (assuming $S=\frac{1}{2}$) $g_d=4.66\pm0.05$. Mrs. Barros also obtained new data along the a' and c directions which yield $g_{a'}=2.65\pm0.09$ and $g_c=4.93\pm0.02$. These values of $g_{a'}$ and g_c are in good agreement with the earlier results and, together with g_d, have been used to diagonalize the g tensor in the a-c plane. We get the principal values $g_1=2.23\pm0.10$ and $g_2=5.13\pm0.03$. Principal axis 1 makes an angle of $-17°\,30'\pm45'$ with the a' direction. In this notation $g_3=g_b=4.90$.

Given this set of principal g values we next attempt to find compatible values of η and η'. Referring to Fig. 5, we see that for $\eta'=-3$, a consistent set of g values corresponds to $\eta=3.25$. Similar consistency is achieved for $\eta'=-4$ with $\eta=3.75$. However, this is not possible for significantly larger or smaller values of η'. Referring now to Fig. 4, we find that these two sets of values of η and η' correspond to rather different relative spacings of the three lowest Kramers doublets. The choice between these schemes must be made so as to give the best description of the specific heat data.

In Fig. 3 the excess heat capacity of $CoCl_2\cdot 6H_2O$ over the lattice contribution is shown for two estimates of the latter. Using unadjusted $NiCl_2\cdot 6H_2O$ data for this purpose we obtain the upper curve whose maximum value $\sim0.82R$ is achieved at ~100°K. We note, however, that the maximum in a Schottky anomaly due to a lower doublet and two upper degenerate doublets amounts only to $0.68R$ while the anomaly due to three equally spaced doublets amounts only to $0.65R$. Thus it appears quite likely that the lattice correction is too small in this case.

The lower curve in Fig. 3 is that obtained using $NiCl_2\cdot 6H_2O$ data adjusted according to the corresponding states argument as the lattice correction. We see that the maximum has been significantly lowered and shifted to a temperature of ~83°K. As was emphasized earlier, the uncertainty accumulated in the subtraction of these sets of large numbers becomes quite large. The conservatively estimated uncertainties are indicated by vertical bars in Fig. 3. Note that maximum values of $0.65R$, exhibited by the Schottky anomaly due to three equally spaced doublets, or of $0.43R$ corresponding to only two doublets, both fall within the range covered by these uncertainties. Thus the magnitude of the excess heat capacity near its maximum or above is not very useful in this case as a source of quantitative information about level separations. The excess heat capacity values given most weight in the fitting of a theoretical curve are those at temperatures below ~60°K.

Before computing the heat capacity due to excited Kramers doublets, we must decide on the magnitude of the spin-orbit coupling constant λ to be used, since η and η' are dimensionless quantities with λ the reducing factor. Several investigations have shown λ for the Co^{++} ion in a crystal to be considerably reduced relative to its free-ion value of -180 cm^{-1}. This reduction is due primarily to covalency and the partial breakdown of the ionic picture. In CoF_2, Kamimura and Tanabe[16] find $\lambda=-157$ cm^{-1}, while for $Co(H_2O)_6^{++}$, Jackson and Rai[17] give $\lambda\approx-134$ cm^{-1}.

While the uncertainty in the excess heat-capacity values precludes the precise determination of a spin-orbit constant in the present case, λ does appear to be smaller than the free-ion value. Guided by the findings for other salts, we have taken $\lambda=-140$ cm^{-1}. With this choice, we find from Fig. 4 that $\eta=3.25$ and $\eta'=-3$ correspond to having the second and third Kramers doublets, respectively, 152 and 630 cm^{-1} above the lowest one. Similarly for $\eta=3.75$ and $\eta'=-4$, we find the corresponding separations amounting to 126 and 761 cm^{-1}.

The electronic contribution to the heat capacity of $CoCl_2\cdot 6H_2O$ has been calculated including in the single-ion partition function all six of the basic group of Kramers doublets. A comparison of the computed Schottky curves with the data indicates that $\eta=3.25$ and $\eta'=-3$ are the more satisfactory choices. In Fig. 6 these curves are shown together with another set calculated with the same values of η and η' but with $\lambda=-180$ cm^{-1}, the free ion value. Note that the effect of reducing λ is to shift the Schottky maximum to lower temperatures and to enhance the high temperature heat capacity. The need for such reduction is suggested by the improved agreement it provides with the data, particularly those at the lowest temperatures.

While the uncertainty in our measured excess heat

[16] H. Kamimura and Y. Tanabe, J. Appl. Phys. 34, 1239 (1963).
[17] L. C. Jackson and R. Rai, Indian J. Phys. 38, 49 (1964).

capacity prevents us from drawing quantitative conclusions from its magnitude near the maximum, it is perhaps significant that this quantity appears to exceed the calculated value. A discrepancy of this nature has recently been shown[18] to occur in Schottky anomalies in systems with strong spin-lattice interactions for which the assumption of separable lattice and spin heat capacities begins to break down. This effect could well occur in a salt containing the Co^{++} ion. It must be remembered, of course, that the g factors on which choice of a level scheme depends so strongly have been determined below 20°K. Temperature variations of atomic spacings and crystal field parameters have been ignored in the preceding analysis. These could also contribute to such a discrepancy at temperatures near 100° or above.

[18] F. Persico and K. W. H. Stevens, Proc. Phys. Soc. (London) 82, 855 (1963); V. F. Sears, *ibid.* 84, 951 (1964).

PHYSICAL REVIEW VOLUME 144, NUMBER 2 15 APRIL 1966

Polaron Energy Spectrum

DAVID M. LARSEN
Lincoln Laboratory, Massachusetts Institute of Technology, Lexington, Massachusetts*
(Received 6 October 1965)

The energy spectrum of a polaron—an electron interacting with the longitudinal-optical phonons of a polar crystal—is studied with particular attention given to the region where the polaron excitation energy closely approaches the energy of a longitudinal-optical phonon. In this region, existing theories of the polaron spectrum are inadequate; in particular, the usual Rayleigh-Schrödinger perturbation theory is shown to be inconsistent. A self-consistent weak-coupling theory is developed, and a variational theory of the polaron spectrum which, for small coupling, reduces to this weak-coupling theory is presented. Whitfield and Puff, and Schultz have conjectured that the polaron energy $EEpR$, bends over and becomes horizontal as the polaron momentum p approaches from below the value at which the polaron excitation energy, $E(p)-E(0)$, becomes equal to the optical-phonon energy. Using the weak-coupling method of the present paper, this conjecture has been verified to lowest order and next higher order in the coupling constant.

INTRODUCTION

THE energy spectrum of an electron in the conduction band of a crystal is usually determined primarily by the detailed form of the periodic potential of the crystal lattice. In many cases the electron energy in the lattice takes the familiar form $p^2/2m$, where p is the electron momentum and m is the so-called "band mass" of the electron, which is characteristic of the periodic lattice and in general not equal to the electron mass in vacuum. If the crystal in question happens to be a polar material, like AgBr or NaCl, the electron will polarize the crystal lattice around it so that in addition to the periodic potential of the lattice, the electron sees a potential due to its induced-polarization charge. The electron plus its associated lattice polarization is called a "polaron." The polaron energy differs from the energy of the electron plus rigid lattice because of the polarization interaction.

It is expected that the lattice modes most strongly affected by the Coulomb field of the electron will be the longitudinal-optical phonon modes. Therefore the study of polarons is the study of the interaction of an electron with the longitudinal-optical phonon modes of the lattice.

The energy $\hbar\omega$ of a longitudinal-optical phonon is approximately independent of phonon wave vector.

* Operated with support from the U. S. Air Force.

If the electron couples very weakly to the longitudinal-optical phonon we would expect the polaron energy to differ only slightly from $p^2/2m$. Let $E(p)$ be the polaron energy. Then we might expect that as p increases, $E(p)$ increases continuously until the polaron excitation energy

$$\mathcal{E}(p)=E(p)-E(0) \tag{1}$$

equals $\hbar\omega$. (Polaron excitation energies will always be denoted by script symbols.) If we define a critical momentum p_c by

$$\mathcal{E}(p_c)=\hbar\omega, \tag{2}$$

we observe that the polaron becomes unstable to optical-phonon emission when $p \geq p_c$. For p less than but very close to p_c, the effects on $E(p)$ due to the electron-phonon interaction should become relatively pronounced. These effects are not properly taken into account in the standard polaron theories.

It is the purpose of this paper to derive a more accurate expression than has been previously available for $\mathcal{E}(p)$ when $p \leq p_c$ and the electron-phonon coupling is not very strong.

WEAK-COUPLING THEORY

Our model for the electron-phonon interaction is defined by the Fröhlich Hamiltonian, given in dimen-